Nonlinear motions at the internal tide source

Hans van Haren[1]

Received 25 January 2006; revised 17 March 2006; accepted 27 April 2006; published 7 June 2006.

[1] Oceanic internal tidal wave generation is commonly modeled via interaction of a sinusoidal barotropic vertical velocity W with topography. However, general w above slopes are predominantly nonlinear, as appears in some nonhydrostatic models. Here, 1–2 Hz sampled observations are presented from 2–84 m above the bottom (mab) at ~1400 m at the Bay of Biscay continental slope. Fronts are observed that all propagate upslope having heights >50 mab and more or less, ±5%, occurring at the tidal periodicity. They are accompanied by O(10 min) pulses of $w \approx 0.10$ m s$^{-1} \gg W$ and irregular small-scale waves superimposed on an asymmetric tidal signal. This nonlinearity is further exemplified by variations in frontal arrival and steepness, height, form, and is causing: i) internal tidal intermittency of ~10 tidal periods, ii) nonlinear generation of internal tidal higher harmonics at the source. The observations suggest internal tide generation in a broadband instead of a monochromatic beam. **Citation:** van Haren, H. (2006), Nonlinear motions at the internal tide source, *Geophys. Res. Lett.*, *33*, L11605, doi:10.1029/2006GL025851.

1. Introduction

[2] Historically, the primary source of internal tidal inertio-gravity waves is the interaction of barotropic tidal currents with topography, whether it be small-scale deep ocean hills [*Bell*, 1975], or, more likely, large-scale topography, notably continental slopes [*Baines*, 1982]. In the vicinity of such topography barotropic tidal currents that are essentially horizontal in open ocean basins attain a vertical component W (mainly dominant M_2). Recently, internal wave-generation modeling has seen more complex development, including the recognition that the conversion rate $C = -\rho_* \langle bW \rangle$, ρ_* a reference density, b buoyancy and $\langle\rangle$ tidal averaging, of barotropic to internal tidal energy will also depend on internal tides generated elsewhere and thus modifying b [*Gerkema et al.*, 2004]. Modification of b can also be caused locally by reflection of incoming waves [e.g., *Ivey and Nokes*, 1989].

[3] For good reason, as barotropic tides are highly deterministic or narrowband, most existing models use linear, sinusoidal motions (of which |W| decreases linearly with height) to initially force internal response. However, the observed response in the ocean (with varying stratification) is generally not so deterministic and internal tides are observed to occur intermittently [*Wunsch*, 1975]. This implies a broadband spectral shape, of which the width is about a tenth of the central frequency whilst comprising 90% of the energy [*van Haren*, 2004, hereinafter referred to as vH04]. This intermittency is still an outstanding problem in ocean modeling. Suggestions have been made associating wind effects with stratification variations thus affecting tidal higher harmonics [*Xing and Davies*, 1997], which may also affect tidal intermittency [vH04].

[4] Internal tides not only occur intermittently but they are also involved in nonlinear processes, and mixing can only be induced from nonlinearly steepened waves. Nonlinear response can result from linear forcing, but only through the interaction with a reflecting surface or via self-advection. This has been shown using non-hydrostatic models, e.g., generating internal solitary waves every tidal cycle in the main pycnocline [*Gerkema*, 2001] and creating higher and lower harmonics from internal wave beams crossing in the interior [*Lamb*, 2004] and between incoming and reflected wave at topography [*Peacock and Tabaei*, 2005].

[5] A possible reason for the difficulty of modeling intermittency may be insufficient interaction of linear waves with (independently) broadband forced background variations in stratification and vorticity [vH04], as most models use a fixed stratification. Non-hydrostatic models show such interaction, but so far runs with these computationally elaborate models have been too short to properly verify band broadening.

[6] In this paper, another possibility will be explored following analysis of fast-sampled observations, showing an inherently nonlinear wave moving up and down a continental slope thereby generating nonlinear internal waves immediately at the source, whereby the sinusoidal barotropic W should be replaced by the general w. The 'remote' generation of the nonlinear source wave may follow from: i/ the asymmetric boundary layer response to up- and downward flow in the stratified water above a sloping bottom causing a tilted interface in the interior [*Weatherly and Martin*, 1978; *MacCready and Rhines*, 1993], and ii/ critical reflection of an internal tide generated elsewhere and causing a bore near the bottom [*Ivey and Nokes*, 1989], or iii/ the generation of a strongly nonlinear solitary wave following adjustment of this (originally linearly) tilted interface moving into shoaling waters [*Vlasenko and Hutter*, 2002]. The shoaling nonlinear wave eventually generates a frontal bore with trailing waves that moves up the slope rapidly [*Hosegood and van Haren*, 2004]. Such a bore will occur every tidal cycle when the interior pycnocline depression and rise are predominantly tidally forced, in addition to a main variation of the pycnocline depth for example via sub-inertial, low-frequency forcing.

[7] The present observations are from a slope in the Bay of Biscay (BB), which is known for nonlinear near-bottom motions occurring at the tidal cycle [*Gemmrich and van Haren*, 2002, hereinafter referred to as GH02]. The area is also an important generation site of internal tide beams, with largest generation between about 400–800 m [*Pingree and New*, 1991; *Gerkema et al.*, 2004] and may be important for

[1]Royal Netherlands Institute for Sea Research, Den Burg, Netherlands.

0094-8276/06/2006GL025851$05.00

Table 1. Mooring Details[a]

Property	Value
Latitude	47° 11.121′N
Longitude	006° 12.179′W
Water depth	1412 m
Local bottom slope	5 ± 0.5°
Deployment	23/04/2005 02:15 UTC
Recovery	25/04/2005 08:10 UTC
Current depths, m	1410, 1340 (AqD), 1327–1406 (ADCP)
Temperature depths, m	1346.5–1410 (N2)
Sampling period, s	0.5(ADCP) - 1(N2,AqD)

[a]N2 denotes NIOZ-2 thermistor string, with nominally 128 sensors every 0.5 m [*van Haren et al.*, 2005], AqD denotes Nortek 2 MHz AquaDopp single point 3-D acoustic current meter, ADCP denotes four-beam RDI 300 kHz Sentinel 3-D acoustic Doppler current profiler with 2 GB memory. The ADCP sampled 80 1 m bins, storing single pings and using a 3.9 m transmission length.

internal wave generation via along-slope currents over rugged topography [*Thorpe*, 1996].

2. Data

[8] For a few days the NIOZ mix-BB002 lander was deployed at a moderately sloping bottom about 1/3 of the distance down the 4500 m deep BB-continental slope (Table 1). CTD observations (above 1750 m) during deployment and recovery showed a local buoyancy frequency of N = 20 ± 5f, f the local inertial frequency, between 1100–1500 m using 50 m vertical smoothing. As a result, the mooring site was supercritical for internal semi-diurnal tidal waves that have a slope of 3.5 ± 0.6°, 0.7 times the bottom slope.

[9] The lander held high-sampling rate 2-Hz ADCP, 1-Hz current meters and 1-Hz temperature sensors, the latter along an 80-m long string below a low-drag buoy. Although the area experiences current speeds up to 0.7 m s^{-1}, mooring deflections were <0.7 m vertically (at the buoy), or <8° tilt, in spite of the rather bulky thermistor string of ≤0.04 m diameter.

[10] High-resolution pressure (P) and tilt information is available from the two current meters. Relatively accurate (<0.0015°C) temperature information comes from the thermistor string. The ADCP sampled single pings, but due to occasionally low scatterers' amounts, small-scale (turbulent) currents inhomogeneous over the beam spread, and reflections off the titanium temperature sensor housings, it regularly gave bad data in the lower 50 m above its head, and almost permanently higher up. As a consequence, the ADCP-data are used for time series' visual comparison with temperature data, whilst spectral analysis is impossible.

[11] All current data are transformed to a coordinate system of (u, v, w) = (along-slope, cross-slope, vertical) currents. Here, w is not defined as bottom-normal like in bottom boundary layer studies, because it is the component in the direction opposite to gravity that is important for internal wave generation.

3. Observations

[12] Each tidal cycle, an asymmetric time series of near-bottom temperature (T) is observed at ~1400 m (Figure 1). This pattern is similar to that observed near the bottom at ~800 m in the same area [GH02] and at ~500 m at the slope of Great Meteor Seamount (GMS) [*van Haren et al.*, 2005]. The gradual rise in temperature is followed by a sudden decrease, which is accompanied by large upslope v ≈ 0.4–0.5 m s^{-1}, near-zero u and vigorous w = 0.05–0.15 m s^{-1} (Figure 1). Higher-up, temperature variations are more irregular, whilst w is less varying with depth. The w-time series displays an asymmetric tidal shape just like near-bottom T, but this w-signal is superimposed with short-term variations ~twice the tidal amplitude.

[13] The sudden decrease in T characterizes a front of more than 50 mab that passes the mooring within minutes (Figure 2). The fact that the associated current is directed up the slope suggests a solibore [*Hosegood and van Haren*, 2004].

[14] Although the temperature (and other) patterns seem to repeat themselves every tidal cycle and Froude number is always large F = $|\mathbf{u}|/Nh = 2 \pm 1$ using scale height h = 100 m (Figures 1 and 2), subtle differences occur in time and duration of frontal passage, its temperature change and the vertical extent and form of the solibore, so that they are never the same (Figures 1 and 3). The times of start of largest temperature decrease are, measured at the lowest

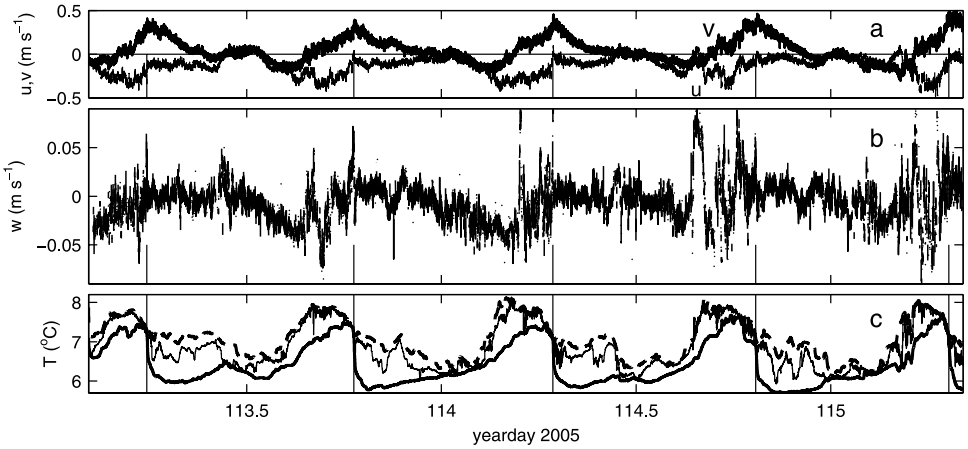

Figure 1. (a) Time series of u(thin), v(heavy; >0 upslope) at 1.7 mab (m above the bottom). (b) 3-s smoothed w at ~25 mab. c. T at 1.7 mab (heavy solid line), 25 mab (thin) and 72 mab (dashed). The five vertical lines indicate the start of passages of steepest 1.7 mab temperature drop in each tidal cycle.

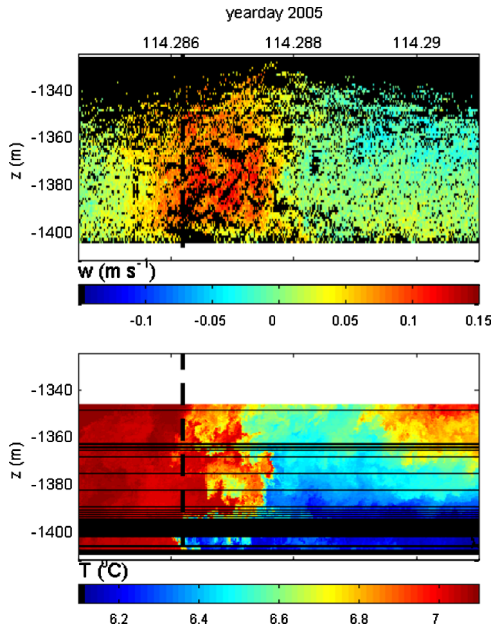

Figure 2. Detailed 10-min view of steepest frontal passage (#3) from (top) unfiltered w (in black are bad data) and (bottom) T (horizontal stripes indicate bad sensors). The vertical dashed line indicates the frontal passage at the lowest temperature sensor.

thermistor: days 113.2433, 113.7750, 114.2862, 114.8069, 115.3034. Although fronts are usually curved with distance from the bottom as a backward breaking wave, the variation in timing of frontal arrival across the entire vertical measurement range is <2 min (0.0015 day). As a result, the periodicity between frontal passages at a fixed position is well-defined. The periods are: 12.76, 12.27, 12.50, 11.92 hours determined to within ±0.05 hours, with a mean of 12.36 ± 0.36 hours. Similar re-analysis of previous 1-Hz thermistor string data yield 12.41 ± 0.48 hours for frontal passages at ∼500 m at a slope of GMS observed during 5.5 days.

[15] The varying periodicity is not a precise fixed value of the dominant tidal constituents, 12.42 and 12.00 hours for M_2 and S_2, respectively, and its variability is also not due to, e.g., spring-neap beat period. Instead, it constitutes a broad band of $0.098M_2$ (for the data presented here) between the 90% confidence borders around the M_2-peak.

[16] This bandwidth is well within one standard deviation of the mean $0.09 \pm 0.02M_2$ found in yearlong BB-observations ∼100 km away from the continental slope [vH04]. In the present data, the sharpest and highest front (day 114.2862) extends above the highest sensor above the bottom, whilst the associated w also extends below the sensor closest to the bottom. As a result, a substantial part of the water column is penetrated by a strong w-pulse of typically 0.1 m s^{-1}, with w/v = 0.3–0.5. This value is much larger than the large-scale tidal W/V = 0.05–0.1 commensurate the bottom slope.

[17] All fronts are preceded (up to 3 hours in advance) by a series of irregular and occasionally overturning high-frequency 'waves' (Figures 1 and 3), in which w is large and u non-zero (in contrast with the frontal passage), whilst v is weakly upslope. All fronts are followed by a varying train of waves at the strongest stratification that caps a bottom 'boundary layer' that, however, seldom becomes

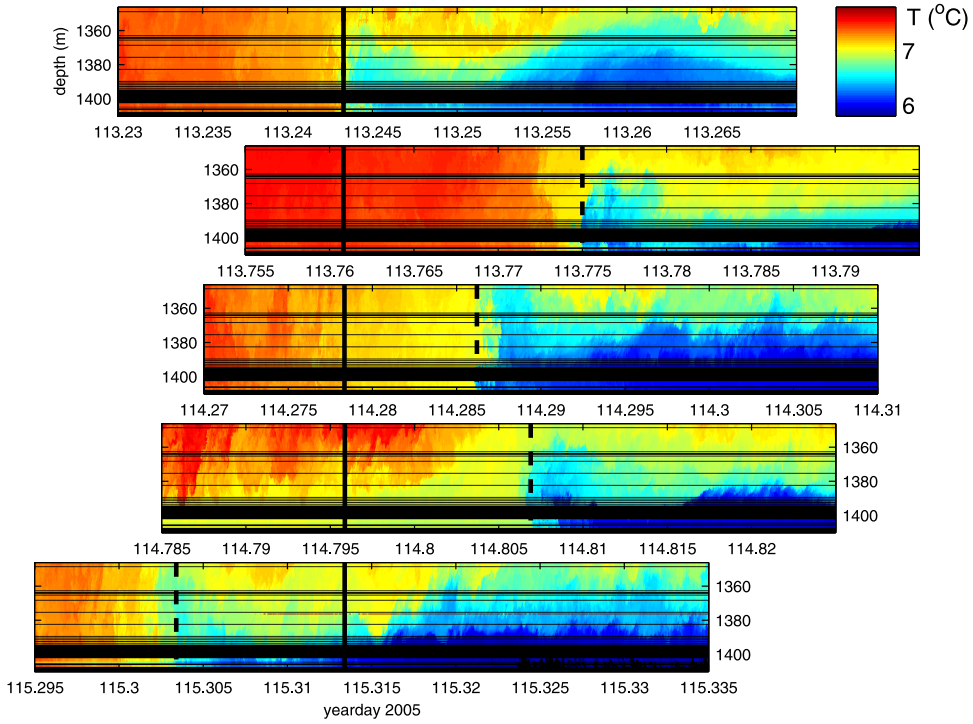

Figure 3. Unfiltered T of all of the five frontal passages in 1-hour panels. The black solid line time reference in each panel is exactly (n-1)·12.42 hours (one M_2 tidal period), n the front number, later than the first front. The dashed lines indicate the true frontal passage at the lowest temperature sensor. The color coding is the same for all panels and slightly different from Figure 2.

fully homogeneous (Figures 1–3). So, although one can hardly speak of a homogeneous boundary layer (Figure 1: T), the main pycnocline found in the vicinity of the bottom is pushed vertically up by the turbulent bore (Figures 2 and 3), and may induce propagating waves starting as interfacial waves from 50–100 mab and onward into the ocean interior. This frontal passage at a main, albeit varying, tidal periodicity causes the following temperature and current spectra [e.g., GH02]: i) a dominant tidal peak, ii) a series of higher tidal harmonics M_4, M_6, etc., iii) [e.g., vH04] finite broad peaks of width of about a tenth of the peak frequencies.

4. Discussion

[18] If we consider the timing of near-bottom frontal passage corresponding with generation of free-propagating internal tidal waves, not just coherent internal tidal motions are generated at deterministic constituent frequencies, but also incoherent tidal motions that determine the broad band and, thus, intermittency in the time domain. As a result, the strongly nonlinear and not strictly deterministic tidally periodic w (and T), as observed at least up to 80 mab, is the source for internal 'tidal' waves, and their higher harmonics, generated above favorable topography. It is suggested that this generation should replace the weaker W as the internal tidal source, even though W may perhaps spread through a larger part of the water column. Of course, longer near-sloping bottom 1-Hz data records above a larger variety of slopes and background conditions are wanted for improved statistics. Further numerical modeling is required on the generation of internal tides via nonlinear w concentrated in the lower ~100 mab, and on the confined beam evolution of a finite bandwidth signal.

[19] Such model may require detailed topographic measurements and it should resolve remote generation and interaction with low-frequency background variations. It may provide insight in variations in timing of arrival and variations in strength of the front along the entire slope, i.e., insight in background-tide interaction. It may also establish effects of low-frequency vorticity on the shut-off of internal tide generation and insight in finite band internal tidal propagation away from the source as a confined group and through varying background conditions. The question is whether a group remains confined, when dissipation balances dispersion [*Thorpe*, 1999], or whether waves at different higher harmonic frequencies directly radiate in different directions from the source [*Peacock and Tabaei*, 2005]. However, in the ocean higher harmonics can also be found in conjunction with enhanced tides (far) away from the internal tide source [*Fu*, 1981; *Xing and Davies*, 2002]. Furthermore, as for varying amplitude in a group, the varying frontal strength observed here suggests rapidly varying amplitude in tidal beams in the interior as well.

[20] Understanding nonlinear internal tide generation and propagation into the interior is important for understanding deep-ocean mixing, also because mixing in the stratified ocean interior and above sloping bottoms can be highly efficient, much more efficient than in homogeneous boundary layers found near the surface and above flat bottoms. High mixing efficiency is a result of a repeated restratification following wave breaking. For example, slow variations in N or low-frequency currents may be brought about following internal mixing due to previous wave passage. As an internal wave beam by definition slopes with respect to the direction of gravity and thus with respect to undisturbed stratification, a simple wave passage already yields an asymmetric wave tilt and thus frontal relaxation, hence possible mixing. This interior mixing widens a pycnocline, which results in a different background state for internal tide generation in the period that follows. It is recalled that C depends strongly on variations in b (N).

[21] **Acknowledgments.** I thank the crew of R/V Pelagia for deployment and recovery of the mooring and Theo Hillebrand and NIOZ-MTM for preparation of instrumentation and mooring. I enjoy continuing discussions on the measurement of internal waves with Theo Gerkema, Leo Maas, Martin Laan and Ruud Groenewegen.

References

Baines, P. G. (1982), On internal tide generation models, *Deep Sea Res.*, *29*, 307–388.

Bell, T. H. (1975), Lee waves in stratified flows with simple harmonic time dependence, *J. Fluid Mech.*, *67*, 705–722.

Fu, L.-L. (1981), Observation and models of inertial waves in the deep ocean, *Rev. Geophys.*, *19*, 141–170.

Gemmrich, J. R., and H. van Haren (2002), Internal wave band eddy fluxes in the bottom boundary layer above a continental slope, *J. Mar. Res.*, *60*, 227–253.

Gerkema, T. (2001), Internal and interfacial tides: Beam scattering and local generation of solitary waves, *J. Mar. Res.*, *59*, 227–255.

Gerkema, T., F. P. A. Lam, and L. R. M. Maas (2004), Internal tides in the Bay of Biscay: Conversion rates and seasonal effects, *Deep Sea Res., Part II*, *51*, 2995–3008.

Hosegood, P., and H. van Haren (2004), Near-bed solibores over the continental slope in the Faeroe-Shetland Channel, *Deep Sea Res., Part II*, *51*, 2943–2971.

Ivey, G. N., and R. I. Nokes (1989), Vertical mixing due to breaking of critical internal waves on sloping boundaries, *J. Fluid Mech.*, *204*, 479–500.

Lamb, K. G. (2004), Nonlinear interaction among internal wave beams generated by tidal flow over supercritical topography, *Geophys. Res. Lett.*, *31*, L09313, doi:10.1029/2003GL019393.

MacCready, P., and P. Rhines (1993), Slippery bottom boundary layers on a slope, *J. Phys. Oceanogr.*, *23*, 5–22.

Peacock, T., and A. Tabaei (2005), Visualization of nonlinear effects in reflecting internal wave beams, *Phys. Fluids*, *17*, 061702.

Pingree, R. D., and A. L. New (1991), Abyssal penetration and bottom reflection of internal tidal energy into the Bay of Biscay, *J. Phys. Oceanogr.*, *21*, 28–39.

Thorpe, S. A. (1996), The cross-slope transport of momentum by internal waves generated by along-slope currents over topography, *J. Phys. Oceanogr.*, *26*, 191–204.

Thorpe, S. A. (1999), On internal wave groups, *J. Phys. Oceanogr.*, *29*, 1085–1095.

van Haren, H. (2004), Bandwidth similarity at inertial and tidal frequencies in kinetic energy spectra from the Bay of Biscay, *Deep Sea Res., Part I*, *51*, 637–652.

van Haren, H., R. Groenewegen, M. Laan, and B. Koster (2005), High sampling rate thermistor string observations at the slope of Great Meteor Seamount, *Ocean Sci.*, *1*, 17–28.

Vlasenko, V. H., and K. Hutter (2002), Transformation and disintegration of strongly nonlinear internal wave by topography in stratified lakes, *Ann. Geophys.*, *20*, 2087–2103.

Weatherly, G. L., and P. J. Martin (1978), On the structure and dynamics of the oceanic bottom boundary layer, *J. Phys. Oceanogr.*, *8*, 557–570.

Wunsch, C. (1975), Internal tides in the ocean, *Rev. Geophys.*, *13*, 167–182.

Xing, J., and A. M. Davies (1997), The influence of wind effects upon internal tides in shelf edge regions, *J. Phys. Oceanogr.*, *27*, 2100–2125.

Xing, J., and A. M. Davies (2002), Processes influencing the non-linear interaction between inertial oscillations, near inertial internal waves and internal tides, *Geophys. Res. Lett.*, *29*(5), 1067, doi:10.1029/2001GL014199.

H. van Haren, Royal Netherlands Institute for Sea Research, P.O. Box 59, NL-1790 AB Den Burg, Netherlands. (hansvh@nioz.nl)